

Sampling Decisions

Michael Chertkov¹, Sungsoo Ahn² and Hamidreza Behjoo¹

Abstract—In this manuscript, we introduce a novel Decision Flow (DF) framework for sampling decisions from a target distribution while incorporating additional guidance from a prior sampler. DF can be viewed as an AI-driven algorithmic reincarnation of the Markov Decision Process (MDP) approach in Stochastic Optimal Control. It extends the continuous-space, continuous-time Path Integral Diffusion sampling technique of [1] to discrete time and space, while also generalizing the Generative Flow Network framework of [2]. In its most basic form – an explicit, Neural Network (NN)-free formulation – DF leverages the linear solvability of the underlying MDP [3] to adjust the transition probabilities of the prior sampler. The resulting Markov process is expressed as a convolution of the reverse-time Green’s function of the prior sampling with the target distribution. We illustrate the DF framework through an example of sampling from the Ising model, discuss potential NN-based extensions, and outline how DF can enhance guided sampling across various applications.

I. SETTING THE STAGE

The overarching goal of **Generative AI** (Gen-AI) is to **generate** samples from a probability distribution, which is represented through **Ground Truth (GT) samples**. A typical Gen-AI model is built upon an exact representation of this distribution using GT samples. For example, in diffusion models where the **score function** governs the generation process, explicit expressions can be formulated as **sums over GT samples**. This is exemplified by the **Iterative Denoising Energy Matching** (iDEM) [4] and **Harmonic Path Integral Diffusion** (H-PID) [1] approaches. These GT-sample-based representations can, in some cases, be powerful enough to generate new samples directly – such as in H-PID, which suggests a form of Gen-AI that operates **without** a Neural Network (NN). Alternatively, the exact GT-sample-based representation of the score function can also be leveraged in a more traditional Gen-AI framework – by training a NN to approximate the exact GT-based expression, as demonstrated in iDEM.

Beyond generative modeling, both iDEM and H-PID also provide AI-driven solutions to a well-established and practically significant problem in statistics: generating independent and identically distributed (i.i.d.)

This work was supported by University of Arizona startup grant.

¹ MC and HB are with Program in Applied Mathematics and Department of Mathematics, University of Arizona, Tucson, AZ chertkov@arizona.edu, hamidreza.behjoo@gmail.com

² SA is with the Graduate School of AI at KAIST, Republic of Korea, sungsoo.ahn@kaist.ac.kr

samples σ from a **target** Gibbs-Boltzmann probability distribution $p(\sigma)$, which is explicitly defined (up to normalization) via an **energy function** $E(\sigma)$:

$$p(\sigma) \propto \exp(-E(\sigma)). \quad (1)$$

Traditionally, this classic sampling problem is addressed using **Markov Chain Monte Carlo** (MCMC).

Moreover, iDEM and H-PID are not the only newly developed AI-based approaches tackling energy-function-based sampling. The **Generative Flow Network** (GFN) framework [2] presents an alternative strategy for sampling from a known energy function, distinguished by two key features:

- **Discrete-Time, Discrete-Space Markov Process:** GFN formulates sampling as a **discrete-time** and **discrete-space** Markov Process (MP), where samples σ are constructed sequentially, starting from an empty state (\emptyset) and progressively growing into a valid i.i.d. sample from Eq. (1)¹.
- **Incremental Sample Growth with History Dependence:** In GFN, sample construction follows an incremental guidance mechanism, wherein each step involves choosing from a list of possible next extensions. Crucially, these choices are **auto-regressive** – depend not only on the most recent addition but also on the entire history of the sample’s growth.

II. OUR CONTRIBUTION

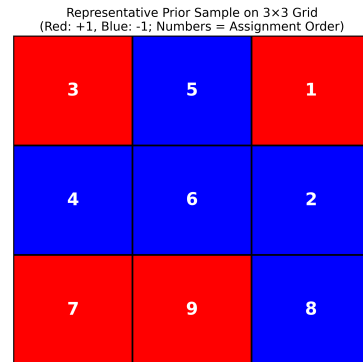


Fig. 1. Representative Ising model samples generated on a 3×3 grid from the prior MP $p^{(\text{prior})}(\bullet|\bullet)$. The red and blue colors indicate spins +1 and -1, respectively. The numbers within each cell show the order in which the spins were assigned during the sampling process.

¹In contrast, both iDEM and H-PID are based on continuous-time, continuous-space diffusion processes, where the sample state evolves within a fixed \mathbb{R}^d dimensional space.

We build Decision Flow (DF) framework which addresses the question of i.i.d. sampling based on the queries of the energy function, $E(\sigma)$, but also on the **prior transition probabilities** quantifying sequential growth of a sample – starting with \emptyset and at each step adding a new component to it, therefore growing a chain: $s_0 = \emptyset \rightarrow s_1 \rightarrow \dots \rightarrow s_T = \sigma$ in T steps (where the number of steps is fixed). To clarify the construction consider an example of assigning binary values (spins) to a cell of a planar lattice, say $n \times n$ lattice, as illustrated in Fig. (1). The initial state is $s_0 = \emptyset$. At the first step we pick one of $T = n^2$ cells, a_1 , and assign to it a spin, $\sigma_{a_1} = \pm 1$, thus generating $s_1 = \sigma_{a_1}$. The process continues so that $s_t = (\sigma_{a_1}, \dots, \sigma_{a_t})$ where $\forall t' \neq t'' \leq t$, $a_{t'} \neq a_{t''}$, then producing the complete sample after T steps, $s_T = \sigma = (\sigma_{a_1}, \dots, \sigma_{a_T})$. Generation of the σ -sample is therefore guided by the vector of prior transition probabilities

$$p^{(\text{prior})} \doteq (p_t^{(\text{prior})}(s_{t+1}|s_t)|t = 0, \dots, T-1), \quad (2)$$

Notice that the prior MP (2) is not necessarily consistent with the target distribution (1) in the sense that the prior marginal distribution built according the Bayes rules:

$$\pi_T^{(\text{prior})}(s_T) = \sum_{s_1, \dots, s_{T-1}} \left(\prod_{t=0}^{T-1} p_t^{(\text{prior})}(s_{t+1}|s_t) \right), \quad (3)$$

where $s_0 = \emptyset$, is not equal to $P(s_T = \sigma)$ defined according to Eq. (1). Our main result is:

Theorem 1 (Decision Flow): *Given an energy function $E(\bullet)$ and a vector of prior transition probabilities $p^{(\text{prior})}$ such that all states with finite $E(\bullet)$ are accessible: (*) A consistent vector of transition probabilities $p^*(\bullet|\bullet)$ – one that results in the marginal probability $\pi_T^*(\bullet)$ constructed according to Eq. (3) with "prior" replaced by "*" and satisfying $\pi_T^*(\sigma) \propto \exp(-E(\sigma))$ – can be obtained as follows:*

$$p_t^*(s_{t+1}|s_t) \propto p_t^{(\text{prior})}(s_{t+1}|s_t) \times \sum_{s'_T} \frac{e^{-E(s'_T)} G_{t+1}(s_{t+1}|s'_T)}{\pi_T^{(\text{prior})}(s'_T)}, \quad (4)$$

where $G_\bullet(\bullet|\bullet)$ is the Green function, initialized as

$$G_T(s_T|s'_T) = \delta(s_T, s'_T), \quad (5)$$

and recursively computed for the time-reversed process governed by the prior transition probabilities:

$$G_t(s_t|s_T) = \sum_{s_{t+1}} p_t^{(\text{prior})}(s_{t+1}|s_t) G_{t+1}(s_{t+1}|s_T), \quad (6)$$

for $t = T-1, \dots, 0^2$.

(**) Moreover, p^* is the optimal solution to the following

²Notice that the Green function is not a proper probability distribution, $\sum_{s_t} G_t(s_t|s_T) \neq 1$.

Markov Decision Process (MDP):

$$\min_{p_{0 \rightarrow T-1}, \pi_{0 \rightarrow T-1}} \mathcal{C}(p_{0 \rightarrow T-1}, \pi_{0 \rightarrow T-1}), \quad (7)$$

where the cost function is defined as:

$$\mathcal{C} = \sum_{t=0}^{T-1} \sum_{s_t, s_{t+1}} \pi_t(s_t) p_t(s_{t+1}|s_t) \log \left(\frac{p_t(s_{t+1}|s_t)}{p_t^{(\text{prior})}(s_{t+1}|s_t)} \right), \quad (8)$$

subject to the dynamics, normalization constraints:

$$\pi_{t+1}(s_{t+1}) = \sum_{s_t} p_t(s_{t+1}|s_t) \pi_t(s_t), \quad (9)$$

$$\sum_{s_{t+1}} p_t(s_{t+1}|s_t) = 1, \quad (10)$$

as well as the marginal probability consistency constraint at $t = T$

$$\pi_T(s_T) \propto \exp(-E(s_T)). \quad (11)$$

Here in Eqs. (9,10) $t = 0, \dots, T-1$ and the initial state is given by $s_0 = \emptyset$.

The proof of Theorem 1 is presented in Section IV and proceeds in two steps. First, we introduce a broader class of MDPs than the one defined by Eqs. (7,8,9,10,11), where the cost function is modified, and the consistency constraint is relaxed. In Theorem 2, we show that this generalized MDP belongs to the class of Linear-Solvable Markov Decision Process (LS-MDP) type discussed in [3], [5], [6]. Second, we leverage the solution of the modified and relaxed MDP to construct a solution for the original MDP, thereby proving Theorem 1.

The practical utility of Theorem 1 is demonstrated in Section V, where we develop an efficient algorithm for refining the prior sampler and present experimental results for sampling from an Ising model on small graphs. Finally, Section VI summarizes our findings and discusses potential applications and future experiments using the DS framework.

In the next section, we return to the discussion of the main highlights of DF and its connections to other approaches in Generative AI, as introduced in Section I.

III. DECISION FLOW FRAMEWORK AND ITS CONNECTIONS TO GFN, H-PID, AND RL

The Decision Flow (DF) framework introduced in this manuscript provides a novel and versatile approach to guided multi-stage sampling, significantly generalizing and unifying existing generative AI methodologies, including **Generative Flow Networks** (GFNs) [2], [7] and **Harmonic Path Integral Diffusion** (H-PID) [1]. In essence, DF formulates the sampling task as a sequential decision-making problem governed by a Markov Decision Process (MDP). This viewpoint highlights both the theoretical underpinnings of DF in Applied Mathematics

– via Stochastic Processes, Statistical Mechanics and Stochastic Optimal Control (SOC) – and its practical connections to the three basic concepts of the GenAI – Auto-Regressive **Transformers**, **Diffusion Models** and **Reinforcement Learning** (RL).

A. Links to Generative Flow Networks

GFNs focus on incrementally constructing samples on a Directed Acyclic Graph (DAG) – therefore **growing a sample in an auto-regressive transformer-style fashion**. The flow-based design ensures that trained Markovian flows satisfy balance conditions — for example, Detailed Balance or Trajectory Balance [8], [9] — so that the target distributions match a target distribution of interest. However, GFNs **do not** explicitly incorporate external **guidance** based on **prior transition probabilities**. DF addresses this gap by introducing priors as domain-specific knowledge or heuristics, which are subsequently refined through optimization.

B. Links to Diffusion Models and Integrable SOC

DF also aligns conceptually with H-PID, a continuous-time, continuous-space approach to sampling that employs **backward-time Green (response) functions** to link final (target) distributions with intermediate states. In DF, these ideas are transposed into a discrete-time, discrete-state (also growing with time) framework by using prior transition probabilities and backward Green functions to achieve consistency with the target distribution. Moreover, DF leverages techniques from **Integrable Stochastic Optimal Control**, following the line of work on **Linearly Solvable MDPs** (LS-MDPs) [3], [5], [6] and **Path Integral Control** [10]. In particular, the pathwise corrections to the prior, reminiscent of continuous diffusion approaches, reflect the same underlying principle: adjusting forward transitions by reference to backward probability flows.

C. Links to MDPs and Reinforcement Learning

DF extends and amplifies connections to the Maximum Entropy (MaxEnt) and Inverse Reinforcement Learning (IRL) ideas. In MaxEnt-based MDPs [11], [12], one imposes an entropy-regularized cost that encourages exploration. GFNs were eventually linked to a deterministic variant of this framework in [7], demonstrating that **adjusting the target reward (prior energy) term to account for reverse probability flows** yields a target Gibbs-Boltzmann distribution. DF follows a comparable principle: it incorporates prior energies that, when corrected, align the target state distribution with the desired Gibbs-Boltzmann form. This correction step also strongly resembles continuous-space denoising diffusion in AI.

From a Reinforcement Learning (RL) perspective, DF can be viewed as a specialized RL scheme that bypasses

explicit definition of actions in favor of directly working with transition probabilities (akin to deterministic MDPs). The entire array of RL methods – from policy optimization to value function approximation [13] – remains applicable, offering a rich toolbox for training or fine-tuning DF in practical settings. When external or historical data is available, DF can bootstrap from these priors, effectively reducing exploration costs and improving sample efficiency. This synergy underscores how DF blends classical SOC formulations with data-driven RL principles.

D. Dynamics is Physical, Not Artificial

Beyond algorithmic details, DF extends the approaches of RL and GFN, establishing a conceptual framework for what we may call Physics-Informed AI (see, e.g., [14] and references therein). Built on a solid mathematical foundation – drawing from stochastic processes, statistical mechanics, and stochastic optimal control – DF offers a principled and powerful means of **integrating** information about the **target distribution** with the **physical growth of a sample**. This approach fundamentally **replaces the notion of artificial time**, as used in diffusion models and other non-RL generative AI frameworks, **with actual physical time**, naturally governing the sample’s evolution from scratch.

IV. LINEARLY SOLVABLE MDPs

In this section, we prove Theorem 1 using Theorem 2, which generalizes results from [3], [5], [6] to accommodate a state space that grows over time. To set the stage for Theorem 2, we introduce a modified cost function:

$$\begin{aligned} \bar{C}(\tau, p_{\tau \rightarrow T-1}, \pi_{\tau \rightarrow T-1}) &\doteq \sum_{s_T} \pi_T(s_T) E^{(\text{prior})}(s_T) \\ &+ \sum_{t=\tau}^{T-1} \sum_{s_t, s_{t+1}} \pi_t(s_t) p_t(s_{t+1}|s_t) \log \left(\frac{p_t(s_{t+1}|s_t)}{p_t^{(\text{prior})}(s_{t+1}|s_t)} \right). \end{aligned} \quad (12)$$

We then define a sequence of MDPs for $\tau = 0 \rightarrow T-1$:

$$\begin{aligned} \Psi_\tau(s) &= \min_{p_{\tau \rightarrow T-1}, \pi_{\tau \rightarrow T-1}} \bar{C}(\tau, p_{\tau \rightarrow T-1}, \pi_{\tau \rightarrow T-1}), \quad (13) \\ \text{s.t.} \quad &\text{Eqs. (9,10) for } t = \tau, \dots, T-1, \\ &\pi_\tau(s_\tau) = \delta(s, s_\tau). \end{aligned}$$

Theorem 2 (Linearly Solvable MDP): (i) *The optimal values of the MDPs in Eq. (13) satisfy the following linear recurrence for $u_\tau(\bullet) \doteq \exp(-\Psi_\tau(\bullet))$:*

$$\begin{aligned} u_\tau(s_\tau) &= \exp \left(-E_\tau^{(\text{prior})}(s_\tau) \right) \\ &\times \sum_{s'_{\tau+1}} p_t^{(\text{prior})}(s'_{\tau+1}|s_\tau) u_{\tau+1}(s'_{\tau+1}), \end{aligned} \quad (14)$$

initialized at $\tau = T$ with $u_T(\bullet) = \exp(-E^{(\text{prior})}(\bullet))$, and evaluated backward in time from $\tau = T$ to $\tau = 0$.
(ii) The optimal transition probabilities for $\Psi_0(\emptyset)$ are:

$$p_t^*(s_{t+1}|s_t) = \frac{p_t^{(\text{prior})}(s_{t+1}|s_t)u_{t+1}(s_{t+1})}{\sum_{s'_{t+1}} p_t^{(\text{prior})}(s'_{t+1}|s_t)u_{t+1}(s'_{t+1})}, \quad (15)$$

for $t = 0, \dots, T-1$. The corresponding marginal probabilities $\pi_{\bullet}^*(\bullet, \bullet)$ are given by Eq. (3), replacing "prior" with "*".

Proof: The proof follows the general framework outlined in [3], [5], [6], adapted to our formulation. Due to space constraints, we provide only key highlights.

Using the Hamilton-Jacobi-Bellman approach, we rewrite Eq. (13) as a sequence of recursive relations, initialized at $\tau = T$ and expressing $\Psi_{\tau-1}(\bullet)$ in terms of $\Psi_{\tau}(\bullet)$. These relations involve summation over s_{τ} and optimization over $p_{\tau}(\bullet, \bullet)$ and $\pi_{\tau}(\bullet)$, which are carried out analytically. Applying the logarithmic transformation $\Psi_{\bullet}(\bullet) \rightarrow u_{\bullet}(\bullet)$ leads to Eq. (14). Finally, extracting the corresponding arg-min expressions results in Eq. (15) and the optimal marginal probabilities. ■

A. Proof of Theorem 1

Proof: We now proceed with the proof of Theorem 1. As in the proof of Theorem 2, we provide only key steps. By combining Eqs. (15,14) from Theorem 2, we obtain:

$$p_t^*(s_{t+1}|s_t) = p_t^{(\text{prior})}(s_{t+1}|s_t) \frac{u_{t+1}(s_{t+1})}{u_t(s_t)}, \quad (16)$$

for $t = 0, \dots, T-1$. On the other hand, Eq. (14) can be rewritten naturally in terms of the backward-time Green (response) functions defined in Eqs. (6,5):

$$u_t(s_t) = \sum_{s_T} G_t(s_t|s_T) e^{-E_T^{(\text{prior})}(s_T)}, \quad (17)$$

for $t = T, \dots, 0$. Substituting Eq. (16) into the corresponding expression for the optimal marginal probability yields:

$$\pi_t^*(s_t) = \frac{u_t(s_t)}{u_0(\emptyset)} \pi_t^{(\text{prior})}(s_t), \quad t = 1, \dots, T. \quad (18)$$

So far in the proof, we have only considered the MDPs in Theorem 2. Now, we establish the connection to the MDP in Theorem 1. The consistency condition (11) in Theorem 1, which ensures that the marginal probability at $t = T$ equals the target probability, corresponds directly to the prior energy term $E(\bullet)$ in the cost function of Theorem 2 defined in Eq. (12)³.

³It is crucial – to prevent singularities and ensure that the formulations the theorems are equivalent – that the prior assigns a strictly positive probability to every state in the target distribution Eq. (1).

Evaluating Eq. (18) at $t = T$ and combining it with Eq. (17) leads to:

$$e^{-E(s_T)} \propto \frac{\pi_T^{(\text{prior})}(s_T) e^{-E_T^{(\text{prior})}(s_T)}}{\sum_{s'_T} G_0(\emptyset|s'_T) e^{-E_T^{(\text{prior})}(s'_T)}}.$$

Inverting this relation gives an explicit expression for $E_T^{(\text{prior})}(\bullet)$ in terms of $E(\bullet)$ and $\pi_T^{(\text{prior})}(\bullet)$:

$$E_T^{(\text{prior})}(s_T) = E(s_T) + \log \pi_T^{(\text{prior})}(s_T) + \text{const.} \quad (19)$$

Combining these results, we arrive at the main statement of the theorem, Eq. (4). The remaining statements of the theorem follow naturally from the explicit transformations derived above. ■

V. EXPLICIT NN-FREE DECISION FLOW ALGORITHM

In this Section we focus on describing a Neural Network (NN) - free explicit DF algorithm, because conceptually all the NN-based implementations of the DF framework which we plan to carry over in the future will be built based on the explicit formulation. We will first provide a general description of the algorithm, then specialize to the example of the Ising model, and finally describe our verification and validation experiments.

Let us choose $E_t^{(\text{prior})}(\bullet) = 0$, $t = 1, \dots, T-1$ and assume that $p_t^{(\text{prior})}(\bullet|\bullet)$, $t = 1, \dots, T-1$ – which provides a plausible prior (e.g., pre-trained model or application specific guidance) – is available. We use it to generate K paths, $\Xi^{(k)} = (s_0 = \emptyset, s_1^{(k)}, \dots, s_T^{(k)}), \dots, k = 1, \dots, K$.

Now our task becomes to build an empirical estimate of the posterior transition probability (4), which we do simply by replacing $p_t^{(\text{prior})}(s_{t+1}|s_t)$ by its empirical counterpart

$$\approx \frac{\# \text{ of paths which hit } s_t \text{ at } t \text{ and } s_{t+1} \text{ at } t+1}{\# \text{ of paths which hit } s_t \text{ at } t},$$

and then utilizing Eqs. (3,5,6).

A. Graphical Model Sampling

In addition to its primary application in drug discovery, the GFN approach has also been tested on a combinatorial optimization problem, where high-probability states emerge through a sequential growth process from an empty set to the desired sample [15]. Specifically, [15] examined the efficiency of growing an independent set over a graph. This example, while more academic than practical, provides a sufficiently rich setting to evaluate GFN performance. Notably, the focus of [15] was not on sampling but rather on solving a combinatorial optimization problem – finding the Maximum Likelihood (ML) independent set. This is somewhat at odds with the original motivation behind GFN –

designed to sample i.i.d. from the target distribution rather than to find the most probable sample⁴.

Since we design DF for sampling and wish to adhere to this objective, we deviate from the approach in [15] and focus on the original problem – sampling i.i.d. from the target distribution. Moreover, we concentrate on sampling from the Ising model rather than an independent set problem considered in [15].

We illustrate the Explicit DF sampling algorithm on the Ising model over an undirected graph $\mathcal{G} = (\mathcal{V}, \mathcal{E})$, where \mathcal{V} and \mathcal{E} are the sets of nodes (vertices) and edges, respectively. Our goal is to generate samples, $\sigma = (\sigma_a = \pm 1 | a \in \mathcal{V})$, i.i.d. from the distribution defined in Eq. (1) with the Ising energy

$$E(\sigma) = - \sum_{(a,b) \in \mathcal{E}} J_{ab} \sigma_a \sigma_b - \sum_{a \in \mathcal{V}} h_a \sigma_a, \quad (20)$$

where the pairwise interaction terms $J = (J_{ab} | (a, b) \in \mathcal{E})$ and singleton biases $h = (h_a | a \in \mathcal{V})$ are assumed to be given. The algorithm is implemented in two steps:

(1) Building MP Prior – $p^{(\text{prior})} = (p_t^{(\text{prior})}(s_{t+1} | s_t) | t = 0, \dots, T-1)$: We construct $p^{(\text{prior})}$ as a MP that generates a sample path Ξ according to the following rule: Define a sequence of partial assignments $s_0 = \emptyset, s_1, s_2, \dots, s_N$, where s_t represents the configuration after t steps and $N = |\mathcal{V}|$. Initialize with $V_0 = \emptyset, E_0 = \emptyset$. At each step $t = 0, \dots, N-1$, choose a new node $a_{t+1} \in \mathcal{V} \setminus V_t$ and assign it a spin $\sigma_{a_{t+1}} \in \{+1, -1\}$ according to $\sigma_{a_{t+1}} \sim \text{softmax}\left(\left\{\tilde{h}_b \sigma_b : b \in \mathcal{V} \setminus V_t, \sigma_b \in \{+1, -1\}\right\}\right)$, where the effective bias is given by $\tilde{h}_b = h_b + \sum_{\substack{a \in V_t \\ (a,b) \in \mathcal{E}}} J_{ab} \sigma_a$. After sampling, update the visited set $V_{t+1} = V_t \cup \{a_{t+1}\}$ and define the new state by $s_{t+1} = (s_t, \sigma_{a_{t+1}})$. The complete sample is then $\sigma = s_N = (\sigma_{a_1}, \sigma_{a_2}, \dots, \sigma_{a_N})$, which is generated by the prior $p_{\text{prior}} = \left\{p_{\text{prior}}(s_{t+1} | s_t)\right\}_{t=0}^{N-1}$ ⁵.

(2) From MP Prior to MDP Posterior: Once the MP prior is built we use it to generate K prior samples and then utilize the general scheme above to devise the empirical expressions for the transition probabilities of the posterior process. Then we generate S posterior samples to validate the method and verify its performance against an exact (for small problems) or MCMC bench-mark.

Experiments with the DF Algorithm:⁶ We test

⁴Our hypothesis is that the authors of [15] chose to apply GFN to the ML problem to align with more standard benchmarks. ML estimation in discrete settings has historically received more attention than the more challenging sampling problem.

⁵Note that although this sequential scheme is inspired by the target Gibbs-Boltzmann distribution Eq. (1) for the Ising model defined in Eq. (20), the prior process itself does not yield i.i.d. samples from $p(\sigma)$.

⁶Code is available at <https://github.com/hamidrezabehjoo/DecisionFlow>.

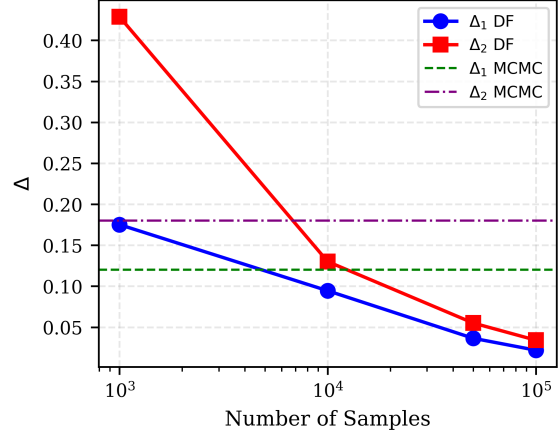


Fig. 2. Performance of the DF algorithm on a 3×3 planar Ising model. Each bias h_a and interaction J_{ab} is independently drawn from Uniform $[-1, 1]$, and the number of prior samples K equals the number of posterior samples S . The plot displays the discrepancy metrics $\Delta_{1,2}$ using the exact reference, as a function of $S = K$. For comparison, dashed horizontal lines indicate results from Metropolis-Hastings MCMC, where the chain discards the first 2000 burn-in samples and then records every 10th sample from a total of 5000 samples.

the DF algorithm on a “glassy” Ising model defined over a planar grid. Fig. 1 illustrates a representative prior sample. Using K prior samples, the DF algorithm generates S posterior (target) samples. To assess sample quality, we compute empirical estimates of the singleton and pairwise correlations:

$$m_a^* = \frac{1}{S} \sum_{s=1}^S \sigma_{T;a}^{(s)}, \quad c_{ab}^* = \frac{1}{S} \sum_{s=1}^S \sigma_{T;a}^{(s)} \sigma_{T;b}^{(s)},$$

and compare them to reference values – obtained either exactly (as in the 3×3 example) or via MCMC. The integrated mismatch metrics are defined as

$$\Delta_1 = \sum_a \frac{\|m_a - m_a^{(\text{ref})}\|}{T \|m_a^{(\text{ref})}\|}, \quad \Delta_2 = \sum_{(a,b)} \frac{2\|c_{ab} - c_{ab}^{(\text{ref})}\|}{T(T-1) \|c_{ab}^{(\text{ref})}\|}.$$

Our results demonstrate that, with a sufficiently small sample size the DF algorithm outperforms MCMC. See Fig. 2 for the Δ -test results and Fig. 3 for the energy probability density function of the generated samples.

VI. CONCLUSIONS AND PATH FORWARD

In this work, we introduced the Decision Flow (DF) framework as a principled approach to guided sampling, bridging concepts from Markov Decision Processes, Generative Flow Networks, and physics-inspired sampling methodologies. By leveraging prior transition probabilities and Green functions, DF enables adaptive corrections that align with a target distribution, offering a powerful alternative to conventional models of GenAI.

Moving forward, we will implement DF using Neural Networks (NNs) to facilitate direct comparison with

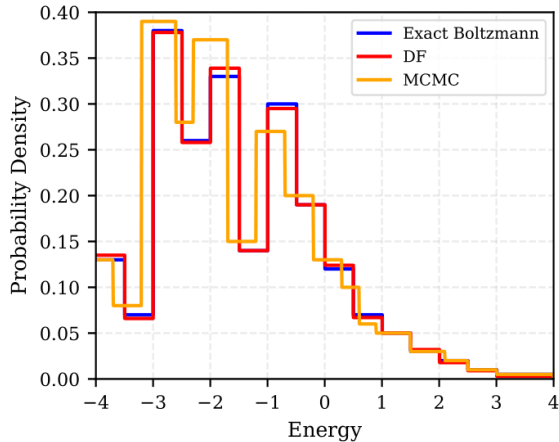


Fig. 3. Probability density function of the energy $E(\sigma)$ estimated from DF-generated samples. The density is computed from σ samples produced using the DF algorithm with $K = S = 5 \times 10^4$, under the same experimental conditions as described in Fig. 2.

state-of-the-art methods such as GFNs. As outlined in Section III, DF holds advantages over existing approaches by explicitly incorporating prior knowledge in a manner that is both theoretically grounded and computationally efficient. The DF framework also stands out in its ability to replace artificial timeline – prevalent in diffusion models – with physical time dynamics, thus enabling more interpretable sampling strategies.

A. Towards New Applications

By establishing DF as a flexible and modular framework, we open avenues for its application across a diverse set of real-world problems where probabilistic sampling plays a crucial role. Below, we highlight key areas where DF can be particularly impactful:

1) *Unit Commitment in Infrastructure Systems:* The DF framework can enhance optimization and control strategies for large-scale systems such as energy and transportation networks. By dynamically adjusting prior transition probabilities, DF can provide robust and scalable solutions for scheduling and resource allocation.

2) *Preventing Outbreaks and Sampling Paths:* In epidemiological modeling, DF enables efficient identification of high-risk pathways for disease spread. By leveraging historical infection patterns and real-time data, DF can assist in mitigating potential outbreaks, whether in viral pandemics or social contagions. The DF methodology extends naturally to agent-based modeling of epidemiological spread. Given a city represented as a geo-graph, DF can adaptively learn and refine transition probabilities, capturing both historical mobility patterns and real-time assessments of infection risk.

3) *Process Control:* Applications in materials science and fluid dynamics stand to benefit from DF’s ability to guide complex processes with embedded physical

constraints. Examples include optimizing reaction pathways in chemical engineering or controlling mixing or temperature in fluids.

In conclusion – uniting theoretical rigor with applications, the DF framework presents a compelling approach to physics-informed AI, offering opportunities for structured sampling in domains where uncertainty, dynamics, and decision-making intersect.

REFERENCES

- [1] H. Behjoo and M. Chertkov, “Harmonic path integral diffusion,” *IEEE Access*, vol. 13, pp. 42196–42213, 2025.
- [2] E. Bengio, M. Jain, M. Korablyov, D. Precup, and Y. Bengio, “Flow Network based Generative Models for Non-Iterative Diverse Candidate Generation,” Nov. 2021. arXiv:2106.04399.
- [3] E. Todorov, “Linearly-solvable Markov decision problems,” in *Advances in neural information processing systems*, vol. 19, pp. 1369–1376, MIT Press, 2007.
- [4] T. Akhound-Sadegh, J. Rector-Brooks, A. J. Bose, S. Mittal, P. Lemos, C.-H. Liu, M. Sendera, S. Ravanbakhsh, G. Gidel, Y. Bengio, N. Malkin, and A. Tong, “Iterated Denoising Energy Matching for Sampling from Boltzmann Densities,” June 2024. arXiv:2402.06121.
- [5] K. Dvijotham and E. Todorov, “A Unifying Framework for Linearly Solvable Control,” Feb. 2012. arXiv:1202.3715.
- [6] M. Chertkov, V. Y. Chernyak, and D. Deka, “Ensemble Control of Cycling Energy Loads: Markov Decision Approach,” Oct. 2017. arXiv:1701.04941.
- [7] T. Deleu, P. Nouri, N. Malkin, D. Precup, and Y. Bengio, “Discrete Probabilistic Inference as Control in Multi-path Environments,” May 2024. arXiv:2402.10309.
- [8] K. Madan, J. Rector-Brooks, M. Korablyov, E. Bengio, M. Jain, A. Nica, T. Bosc, Y. Bengio, and N. Malkin, “Learning GFlowNets from partial episodes for improved convergence and stability,” June 2023. arXiv:2209.12782.
- [9] H. Jang, M. Kim, and S. Ahn, “Learning Energy Decompositions for Partial Inference of GFlowNets,” Oct. 2023. arXiv:2310.03301.
- [10] H. J. Kappen, “Path integrals and symmetry breaking for optimal control theory,” *Journal of Statistical Mechanics: Theory and Experiment*, p. P11011, 2005.
- [11] B. D. Ziebart, A. L. Maas, J. A. Bagnell, and A. K. Dey, “Maximum Entropy Inverse Reinforcement Learning,” in *Proceedings of the 23rd AAAI Conference on Artificial Intelligence (AAAI-08)*, pp. 1433–1438, AAAI Press, 2008.
- [12] S. Levine, “Reinforcement Learning and Control as Probabilistic Inference: Tutorial and Review,” May 2018. arXiv:1805.00909.
- [13] R. S. Sutton and A. G. Barto, *Reinforcement Learning: An Introduction*. The MIT Press, second ed., 2018.
- [14] M. Chertkov, “Mixing artificial and natural intelligence: from statistical mechanics to AI and back to turbulence,” *Journal of Physics A: Mathematical and Theoretical*, vol. 57, p. 333001, Sept. 2024.
- [15] D. Zhang, H. Dai, N. Malkin, A. Courville, Y. Bengio, and L. Pan, “Let the Flows Tell: Solving Graph Combinatorial Optimization Problems with GFlowNets,” Nov. 2023. arXiv:2305.17010.